Supplementary Table 1. Antibodies / Tetramer reagent used in flow cytometry.

No.	Antibody	Clone	Manufacturer
1.	CD45	30-F11	BD Biosciences
2.	CD3	17A2	BD Biosciences
3.	CD4	RM4-5	BD Biosciences
4.	CD8	53-6.7	Biolegend
5.	CD11b	M1/70	Biolegend
6.	CD19	6D5	Biolegend
7.	CD49b	DX5	BD Biosciences
8.	PVRL2	829038	R&D Systems
9.	PVR	TX56	Biolegend
10.	CD11c	HL3	BD Biosciences
11.	CD206	C068C2	Biolegend
12.	Ly-6C	AL-21	BD Biosciences
13.	Ly-6G	1A8	BD Biosciences
14.	I-A/I-E	M5/114.15.2	BD Biosciences
15.	Interferon-γ	XMG1.2	BD Biosciences
16.	TNF-α	MP6-XT22	eBioscience
17.	Foxp3	FJK-16s	eBioscience
18.	H-2 Kb OVA tetramer	SIINFEKL	MBL International

Figure S1

A

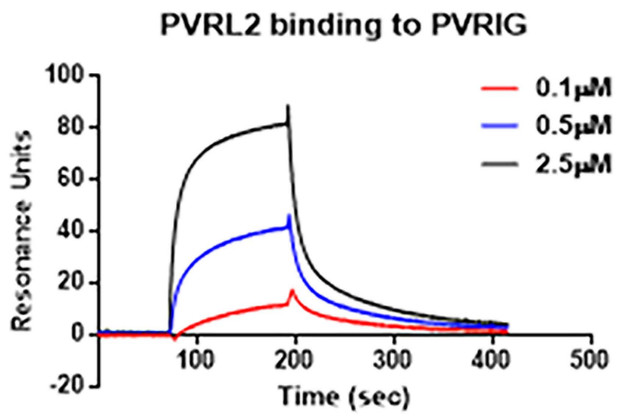

B

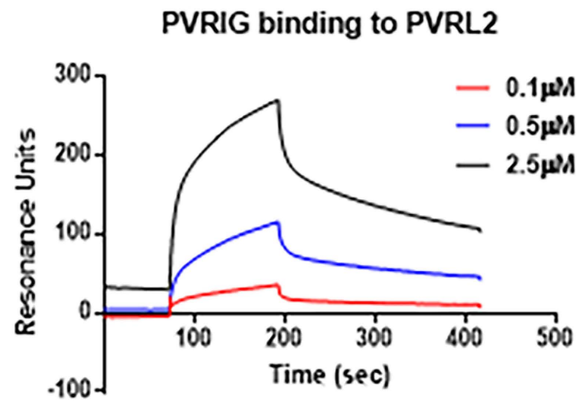

C

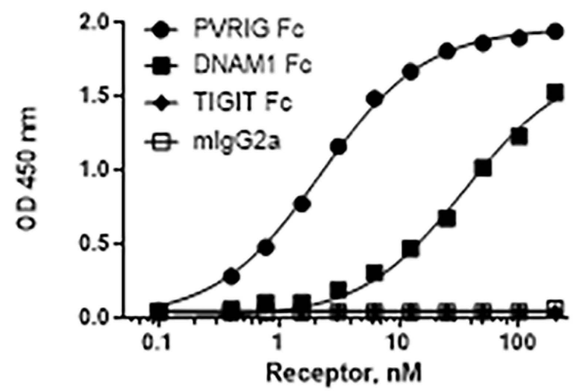

D

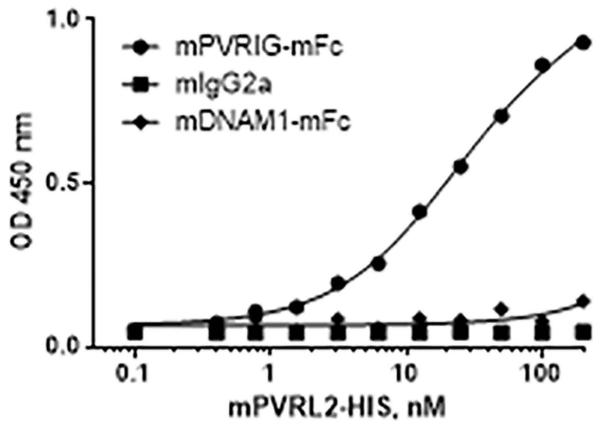

E

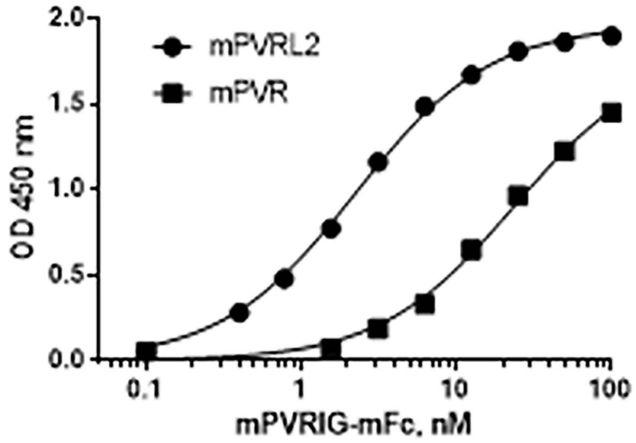

F

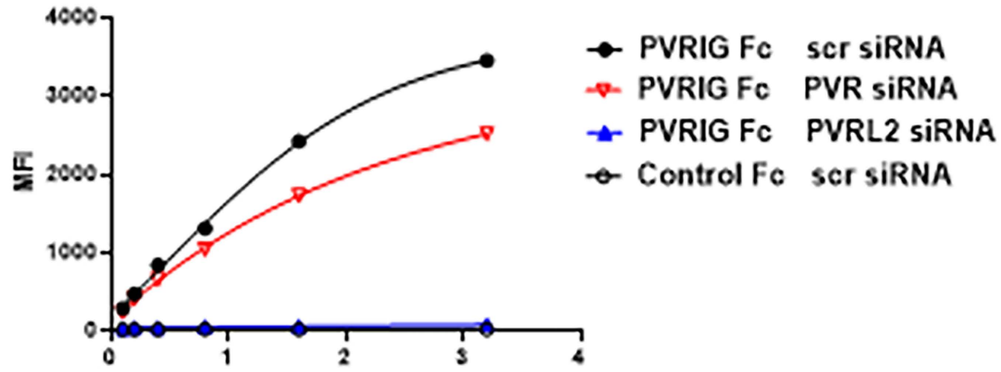

G

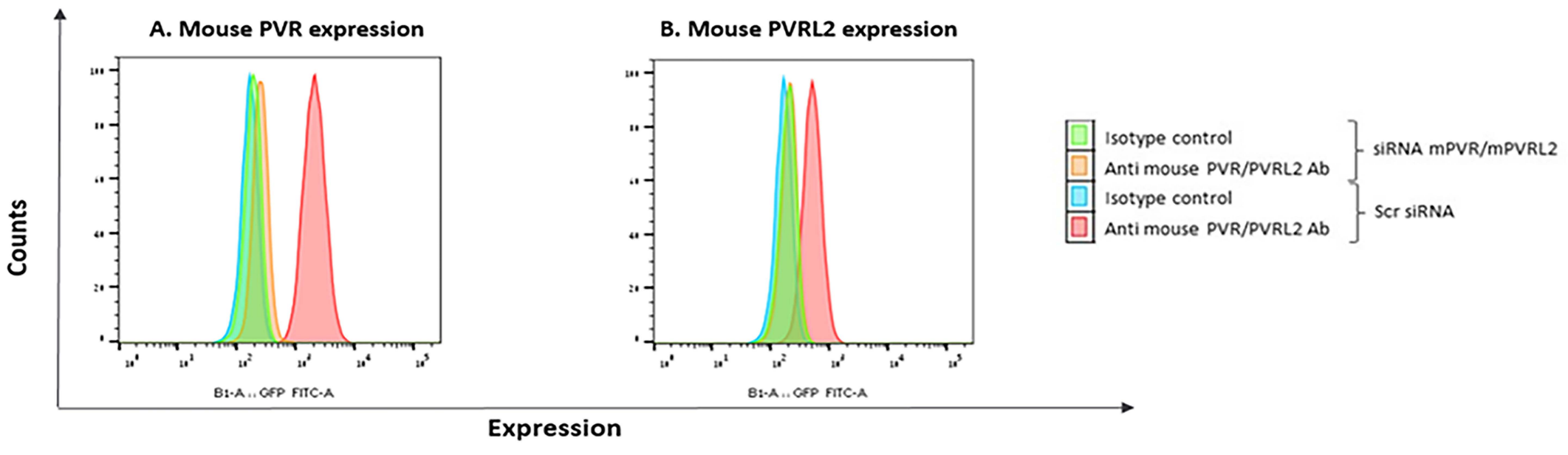

Figure S2

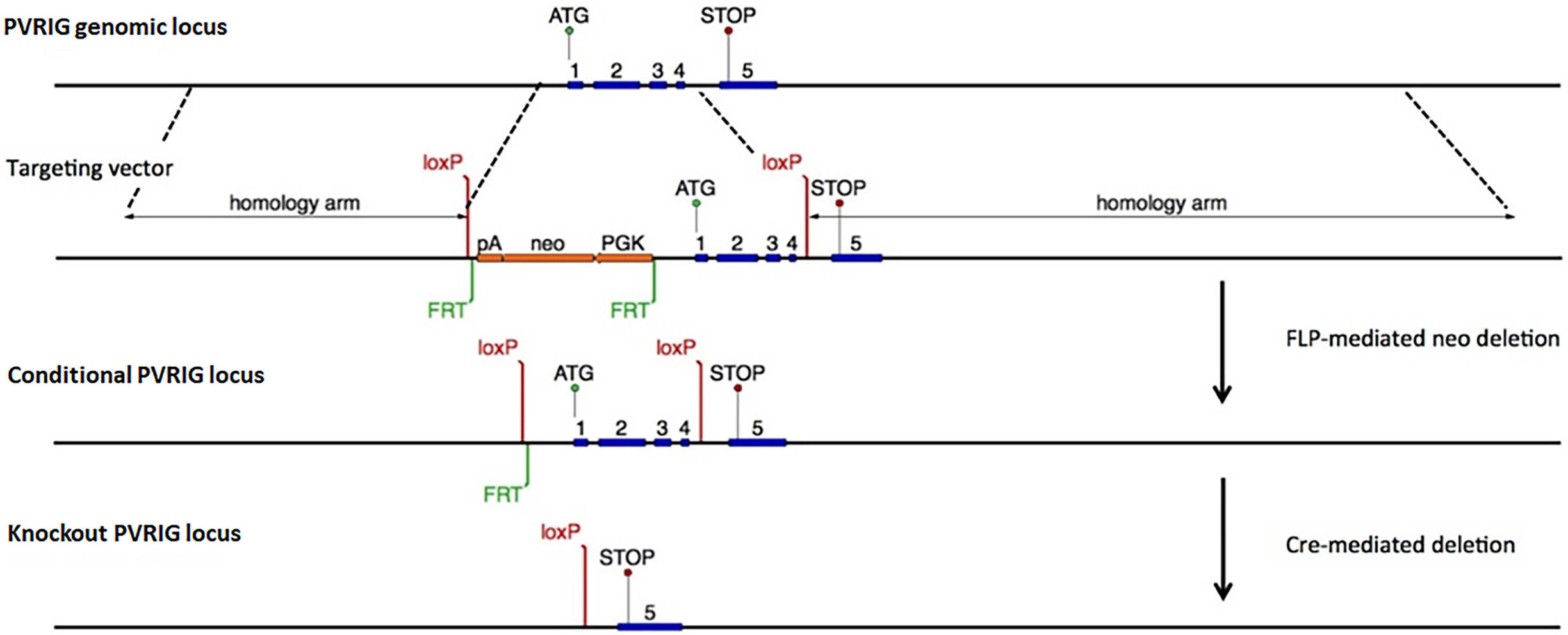
PVRIG genomic locus
ATG
STOP
1
2
3
4
5
Targeting vector
loxP
loxP
homology arm
ATG
STOP
homology arm
pA
neo
PGK
1
2
3
4
5
FRT
FRT
FLP-mediated neo deletion
Conditional PVRIG locus
loxP
loxP
ATG
STOP
1
2
3
4
5
FRT
Knockout PVRIG locus
loxP
STOP
5
Cre-mediated deletion

Figure S3

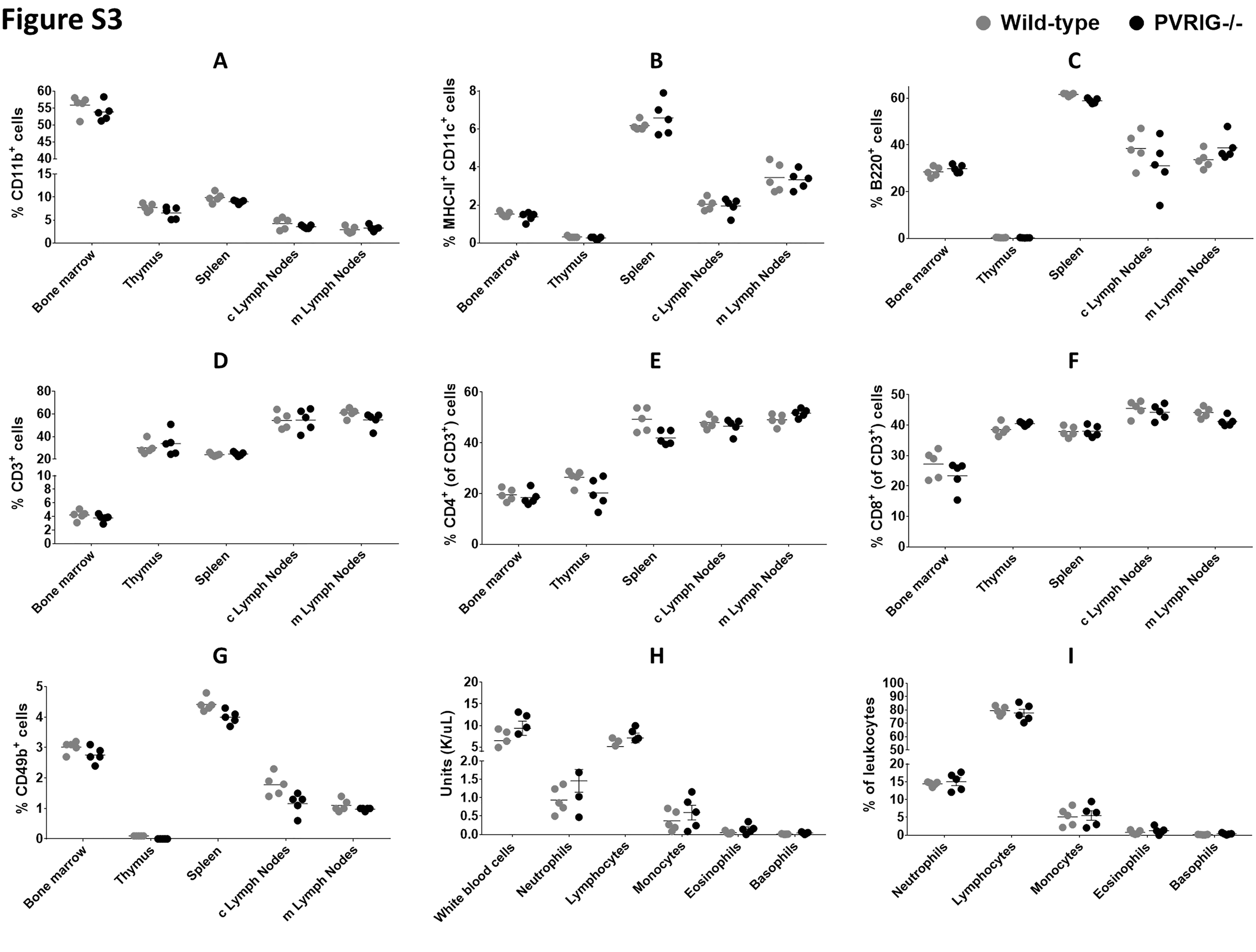
Wild-type
PVRIG-/-
A
% CD11b+ cells
Bone marrow
Thymus
Spleen
c Lymph Nodes
m Lymph Nodes
B
% MHC-II+ CD11c+ cells
C
% B220+ cells
D
% CD3+ cells
E
% CD4+ (of CD3+) cells
F
% CD8+ (of CD3+) cells
G
% CD49b+ cells
H
Units (K/uL)
White blood cells
Neutrophils
Lymphocytes
Monocytes
Eosinophils
Basophils
I
% of leukocytes

Figure S4

A

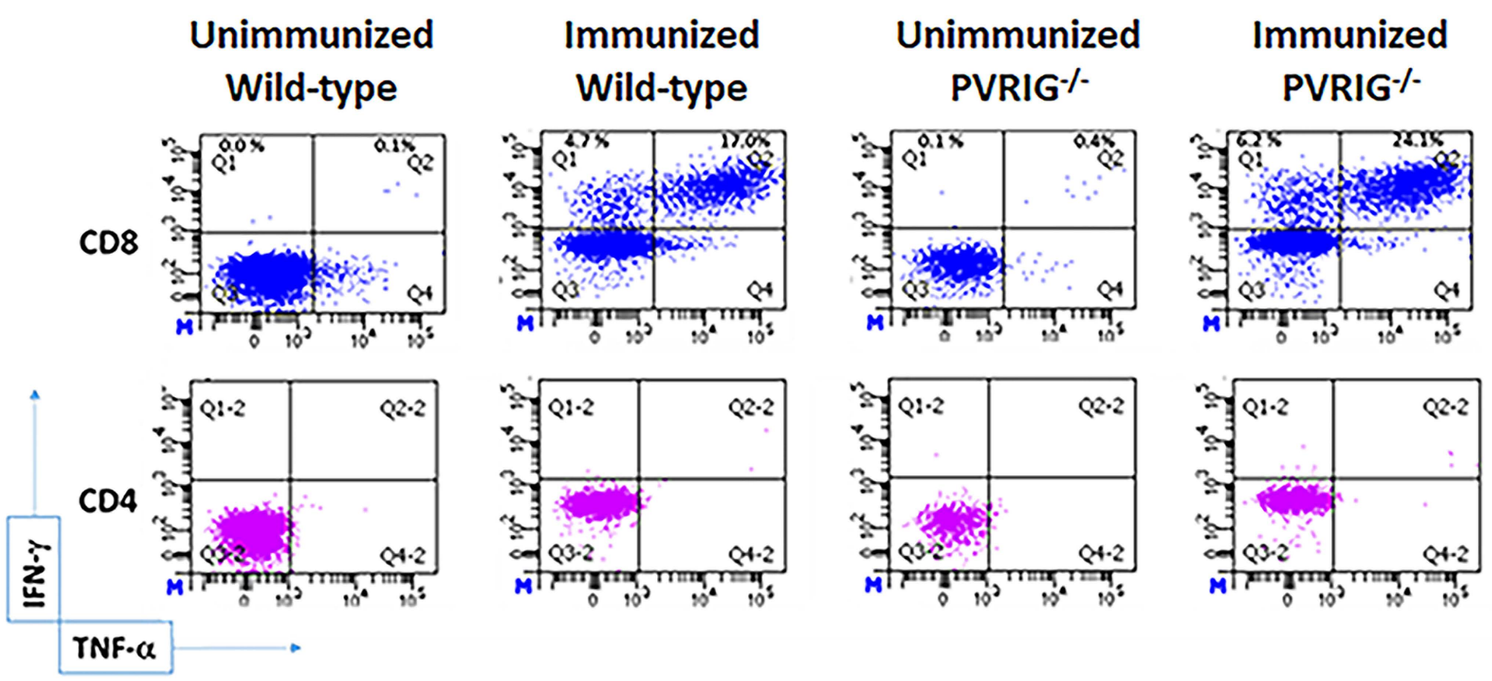

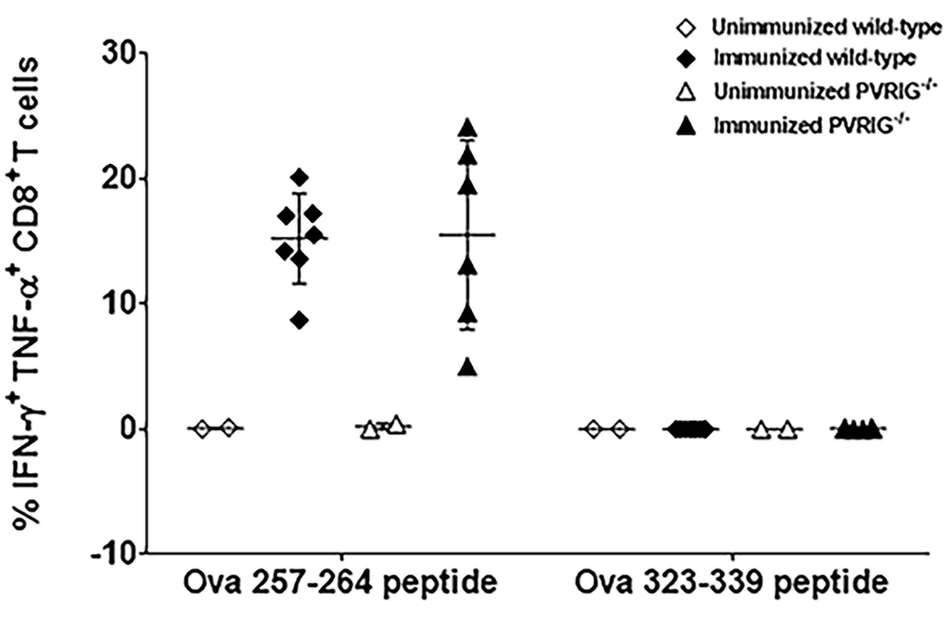

B

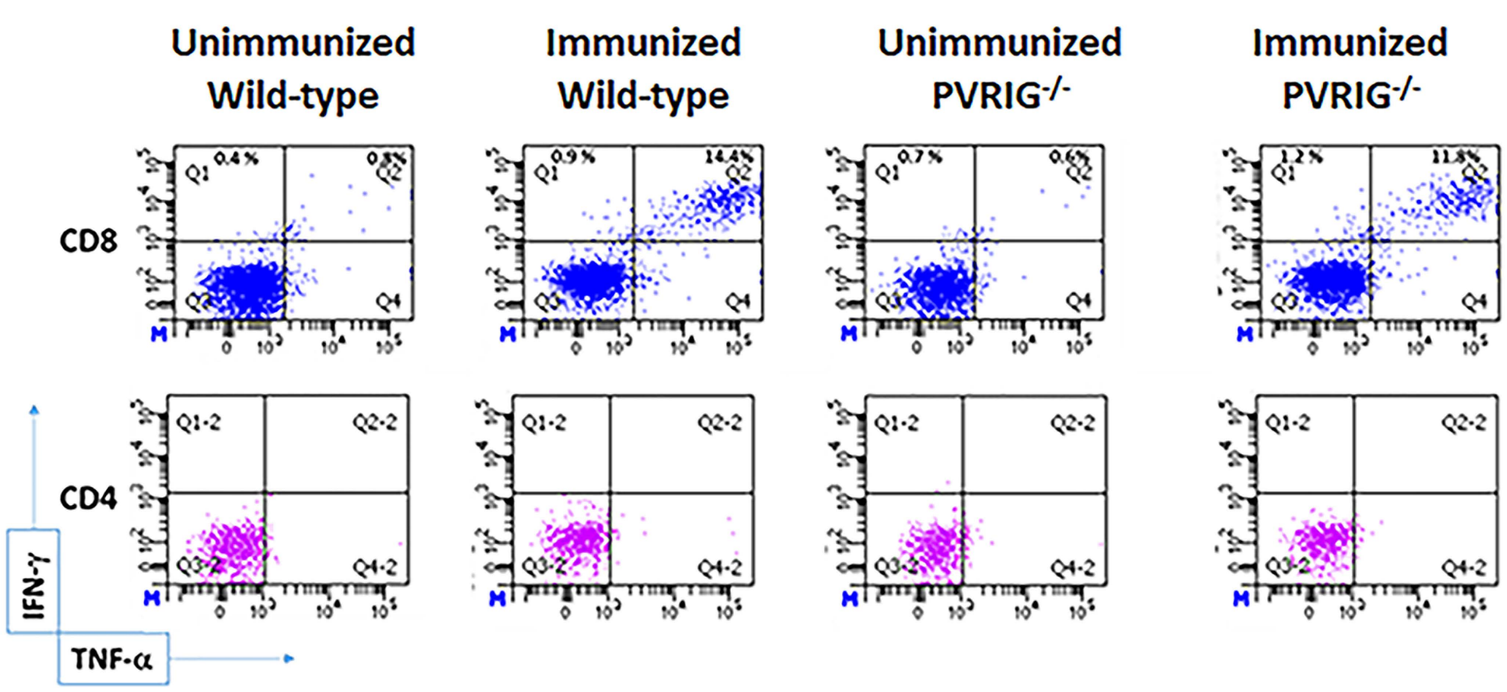

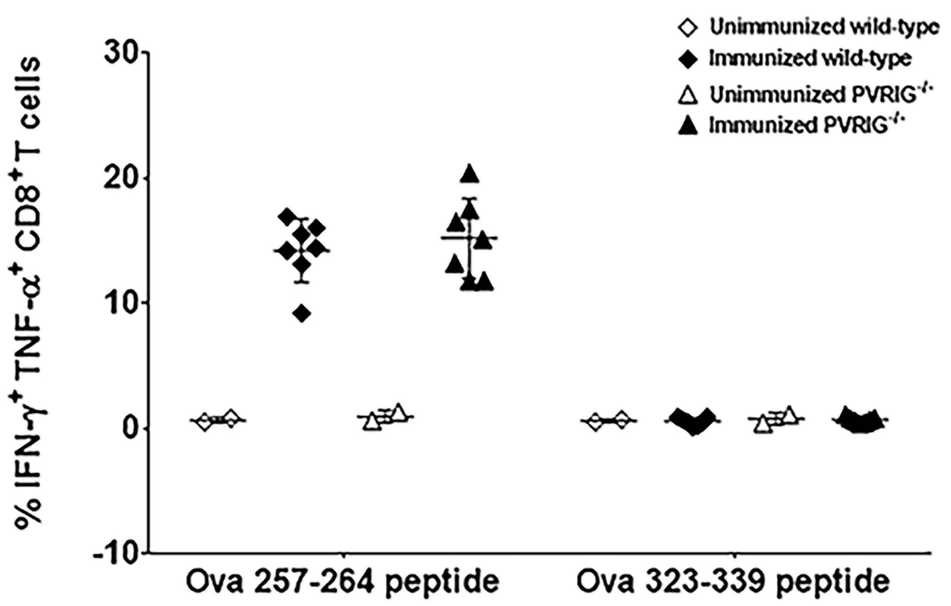

C

Figure S5

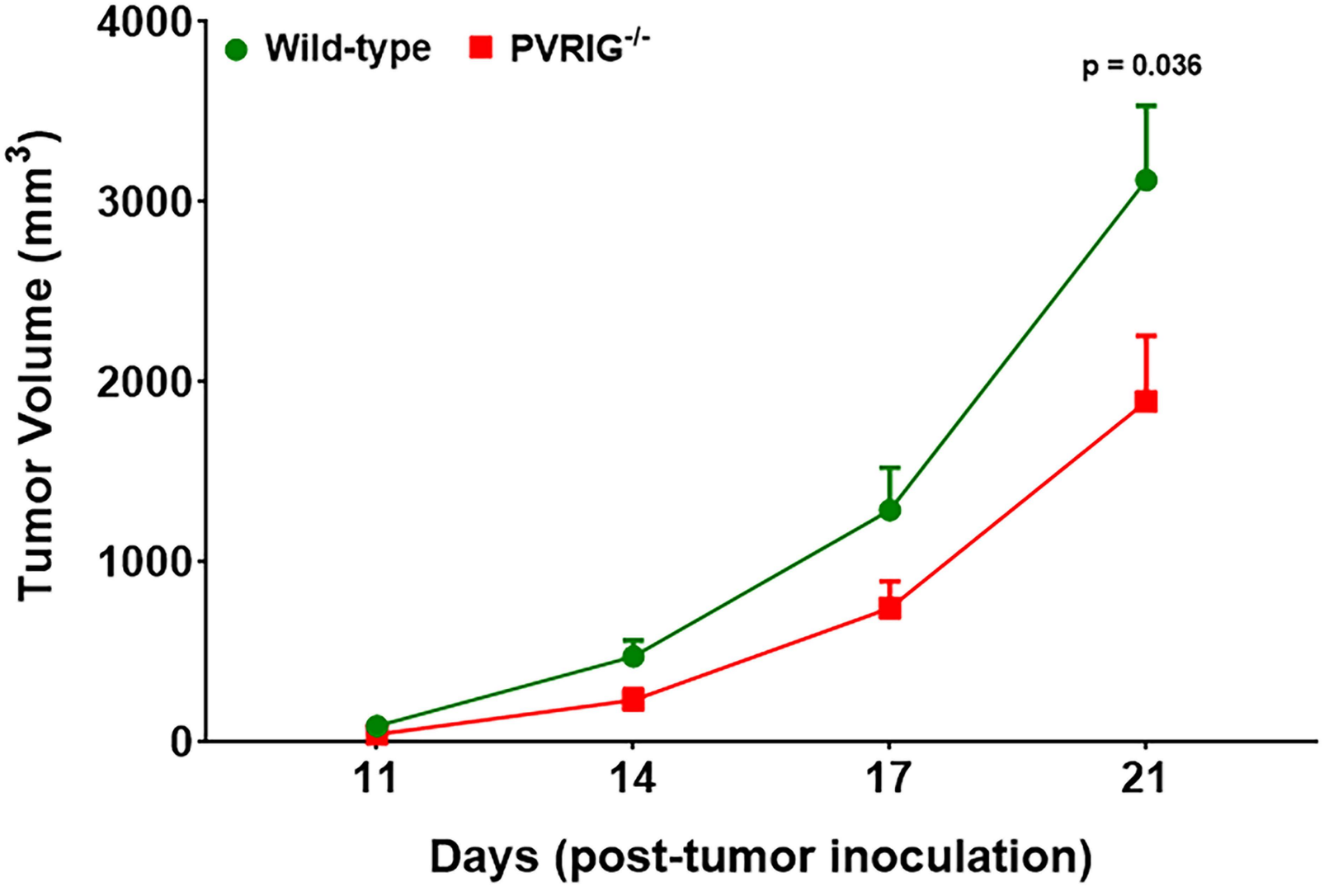
Wild-type
PVRIG-/-
p = 0.036
Tumor Volume (mm3)
4000
3000
2000
1000
0
11
14
17
21
Days (post-tumor inoculation)

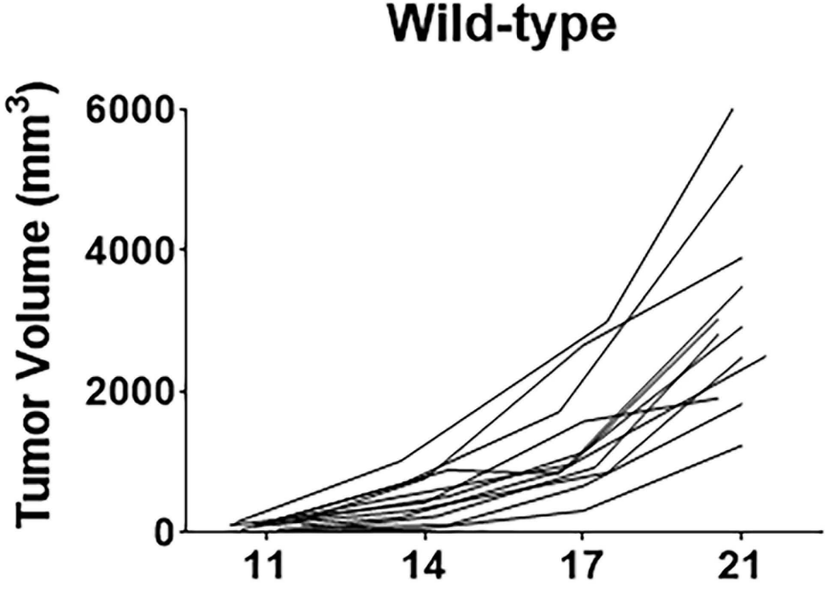
Wild-type
Tumor Volume (mm3)
6000
4000
2000
0
11
14
17
21

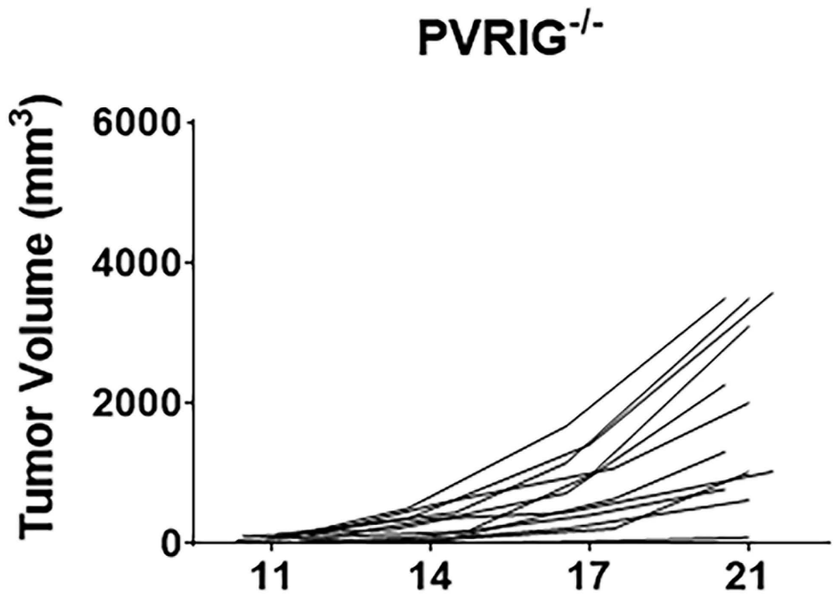
PVRIG-/-
Tumor Volume (mm3)
6000
4000
2000
0
11
14
17
21

Figure S6

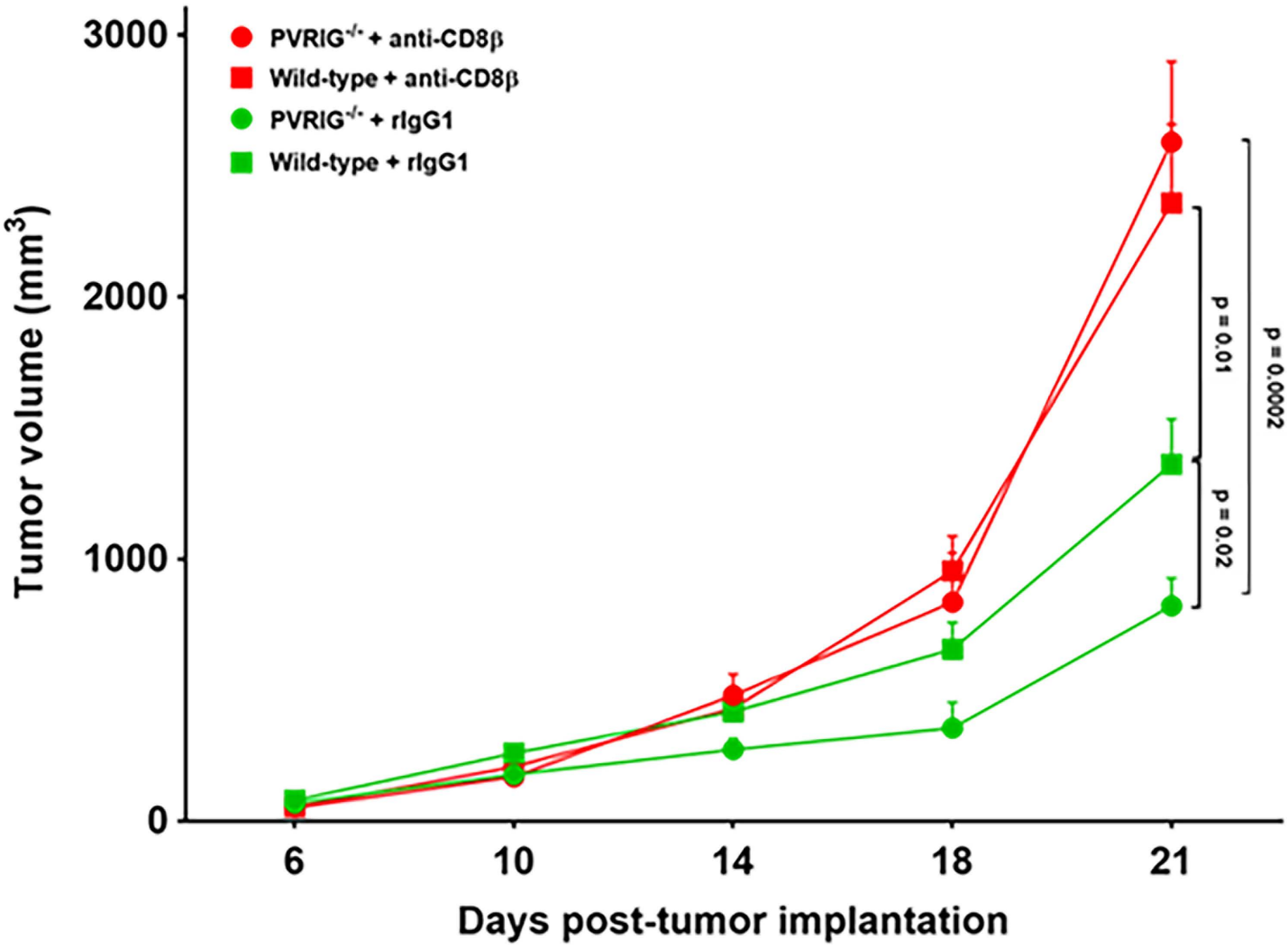
PVRIG-/- + anti-CD8β
Wild-type + anti-CD8β
PVRIG-/- + rIgG1
Wild-type + rIgG1
Tumor volume (mm3)
3000
2000
1000
0
6
10
14
18
21
Days post-tumor implantation
p = 0.01
p = 0.02
p = 0.0002

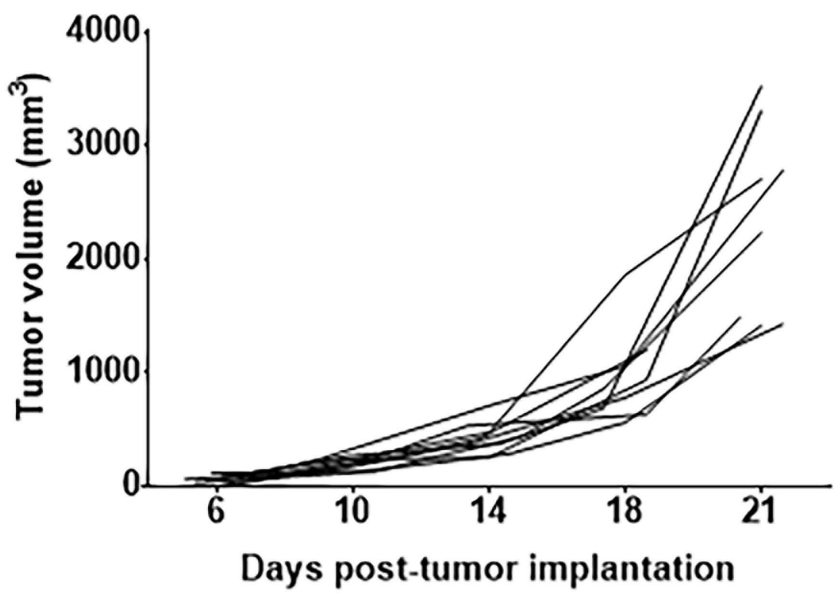
Wild-type + anti-CD8β
Tumor volume (mm3)
4000
3000
2000
1000
0
6
10
14
18
21
Days post-tumor implantation

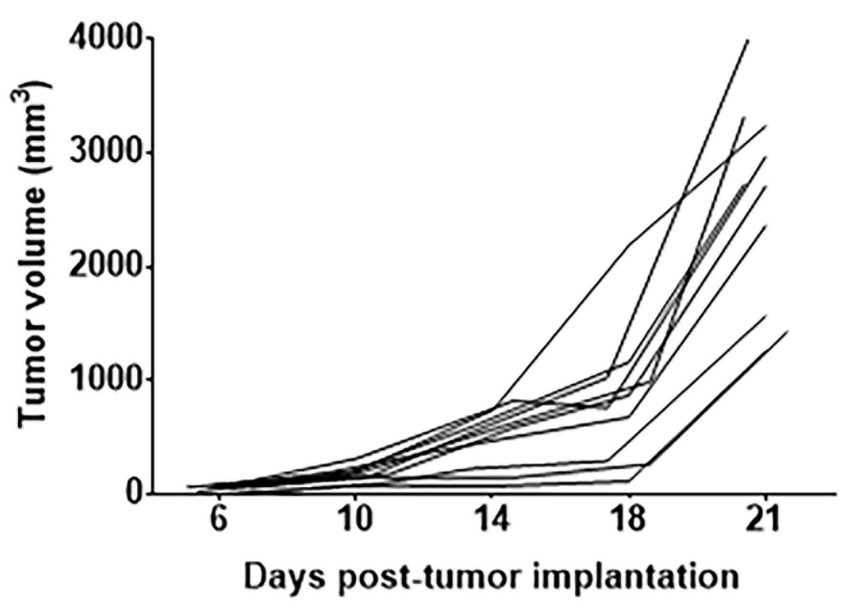
PVRIG-/- + anti-CD8β
Tumor volume (mm3)
4000
3000
2000
1000
0
6
10
14
18
21
Days post-tumor implantation

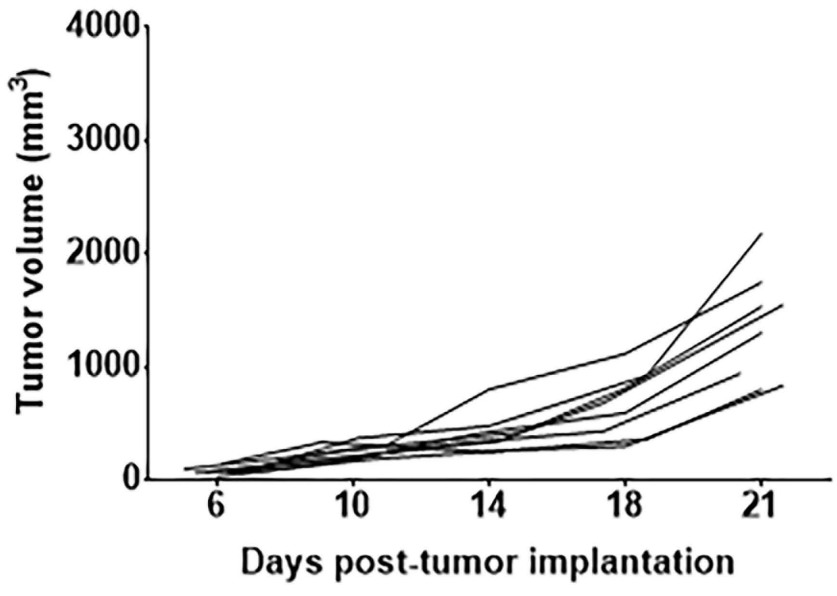
Wild-type + rIgG1
Tumor volume (mm3)
4000
3000
2000
1000
0
6
10
14
18
21
Days post-tumor implantation

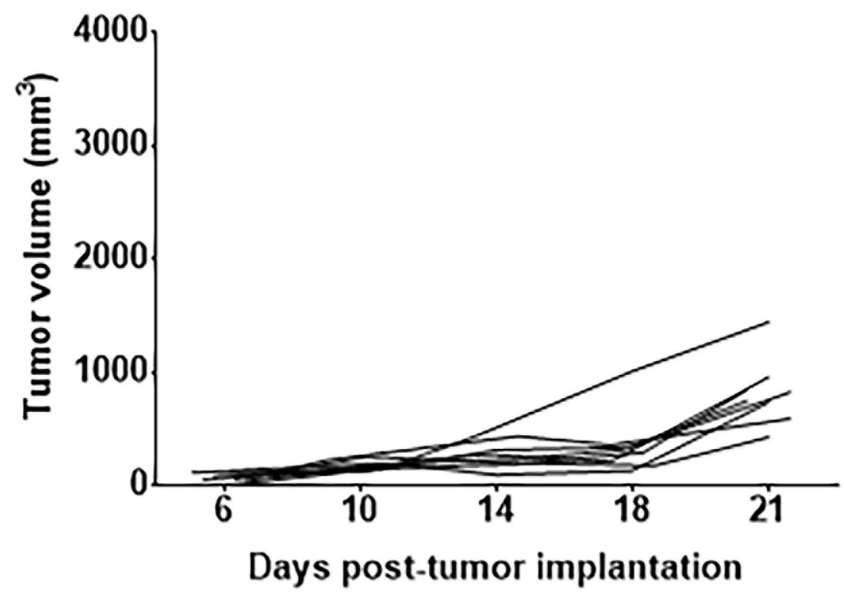
PVRIG-/- + rIgG1
Tumor volume (mm3)
4000
3000
2000
1000
0
6
10
14
18
21
Days post-tumor implantation

Figure S7

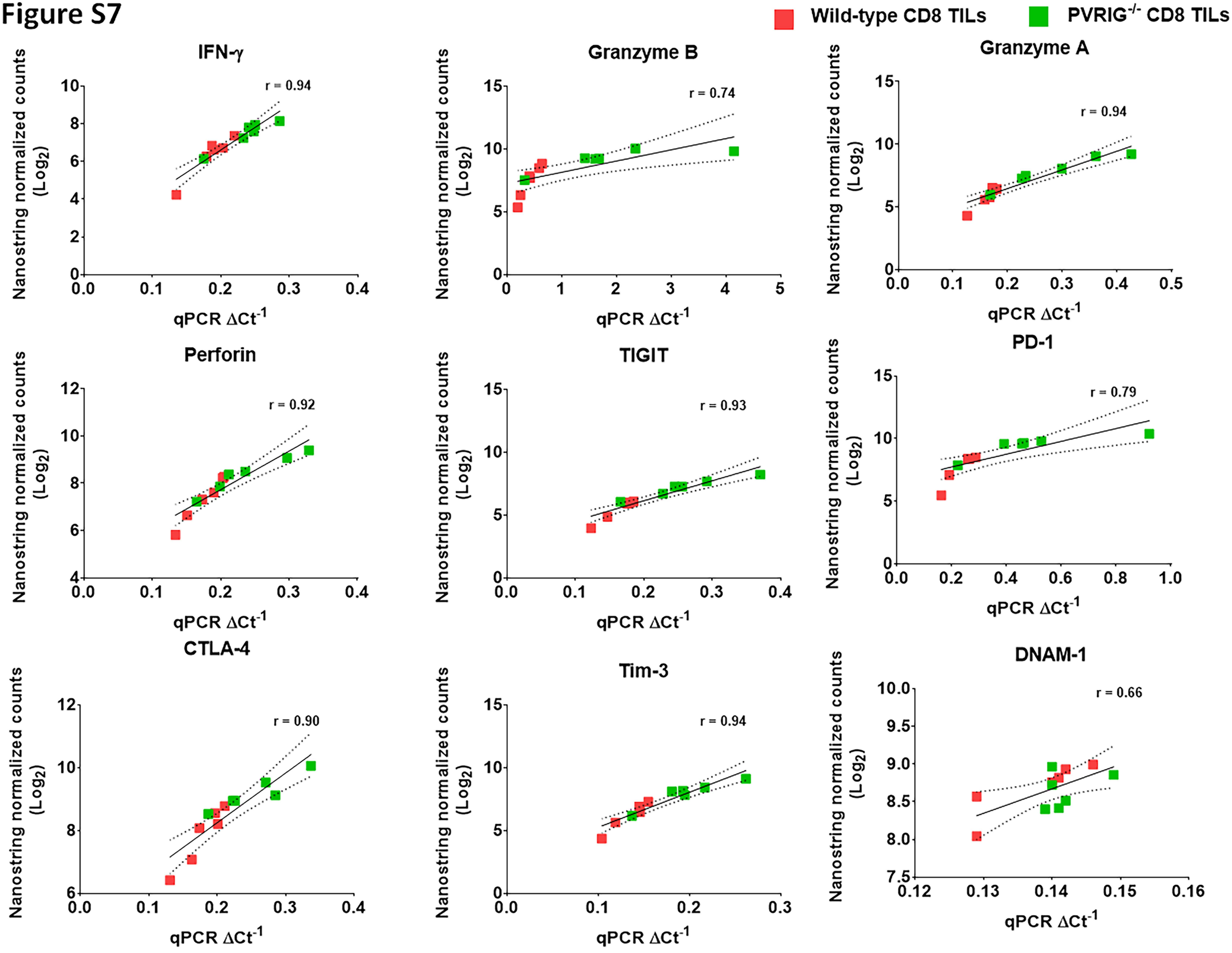
Wild-type CD8 TILs
PVRIG-/- CD8 TILs
IFN-γ
r = 0.94
Granzyme B
r = 0.74
Granzyme A
r = 0.94
Perforin
r = 0.92
TIGIT
r = 0.93
PD-1
r = 0.79
CTLA-4
r = 0.90
Tim-3
r = 0.94
DNAM-1
r = 0.66
Nanostring normalized counts (Log2)
qPCR ΔCt-1

Figure S8

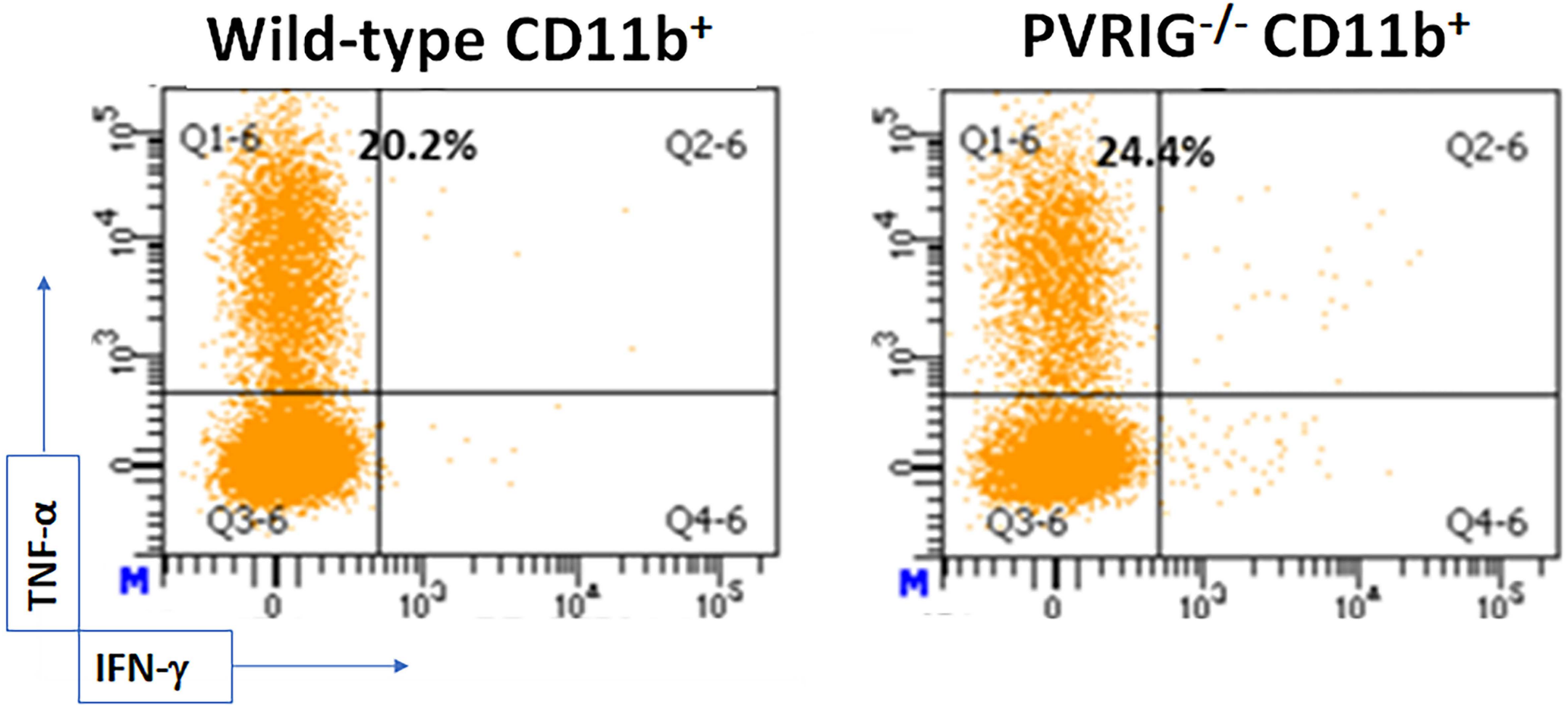
Wild-type CD11b+
PVRIG-/- CD11b+
Q1-6
20.2%
Q2-6
Q3-6
Q4-6
24.4%
TNF-α
IFN-γ
M
0
10³
10⁴
10⁵
% TNF-α+ CD11b+ cells
Wild-type
PVRIG-/-
p =0.02
30
20
10
0
Non-draining LN
Tumor-draining LN
Spleen
Tumor

Figure S9

A

PVRIG-/-

Wild-type

CD11b+ gate

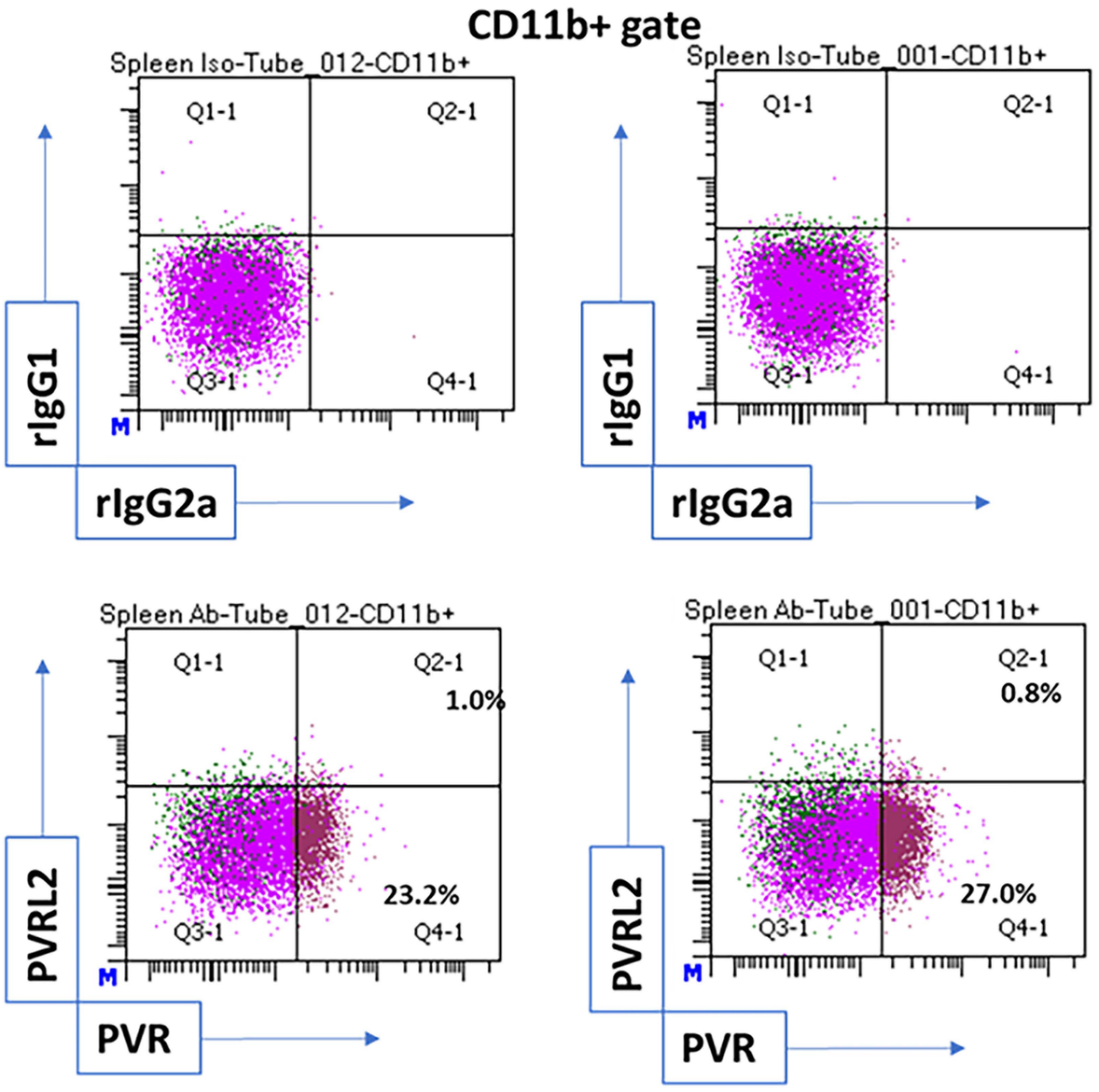

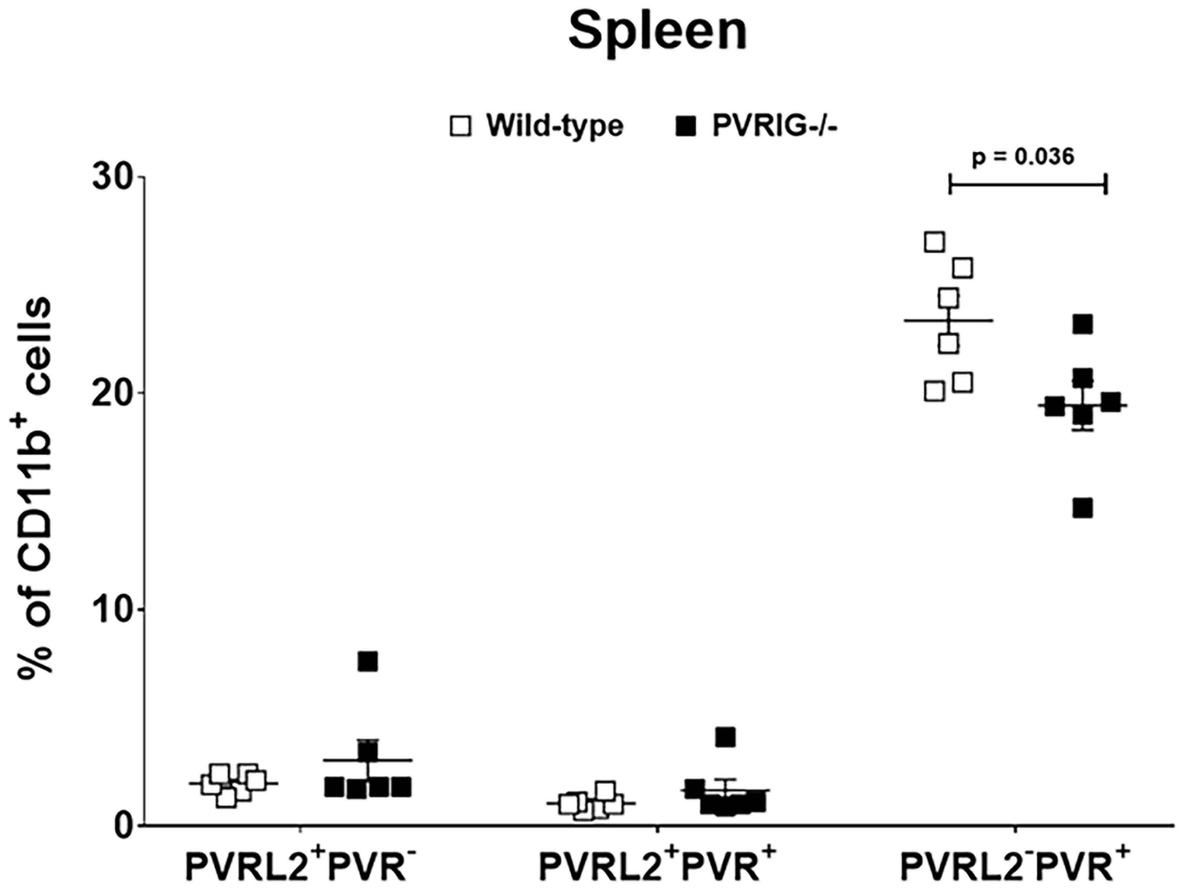

B

PVRIG-/-

Wild-type

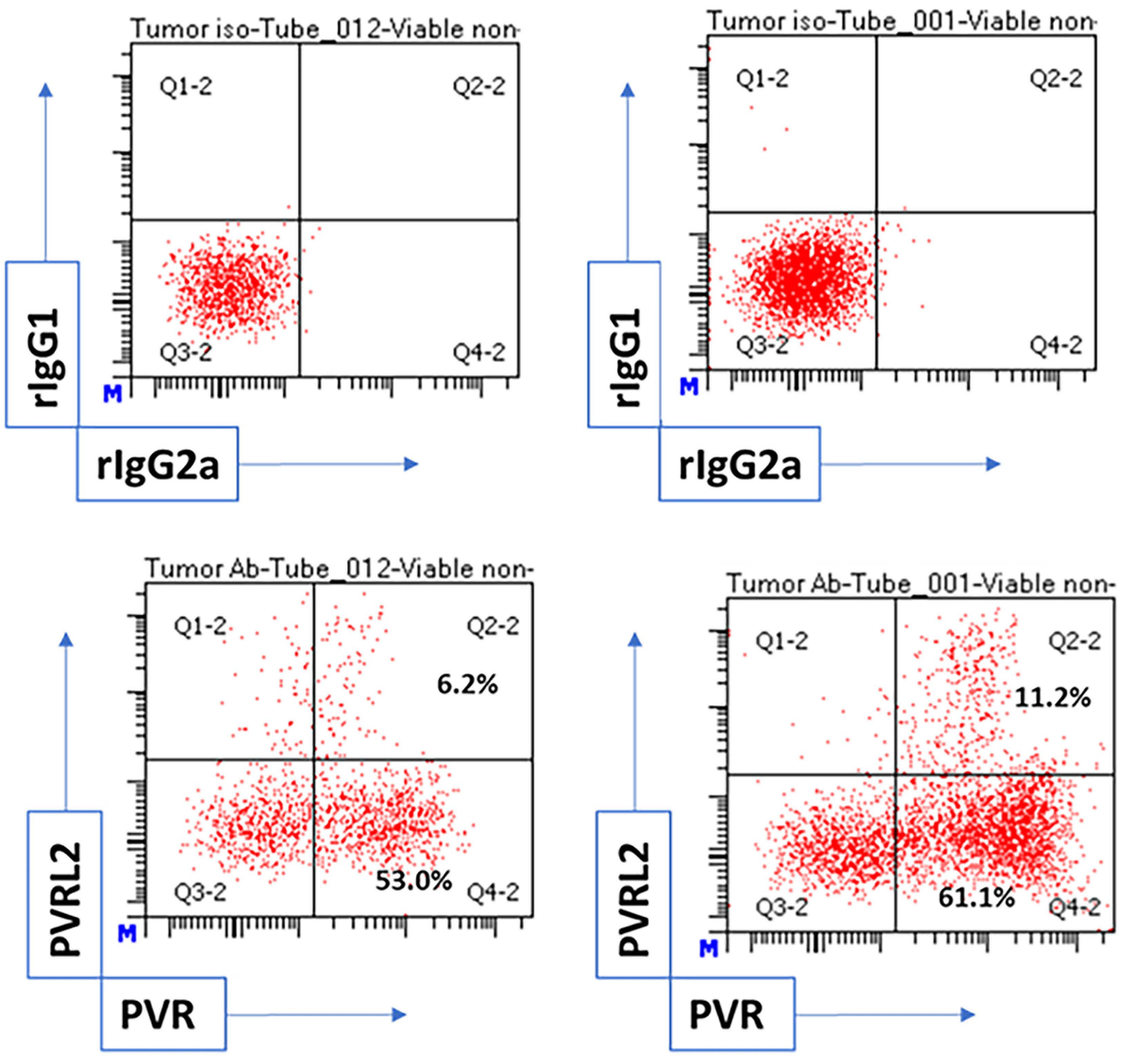

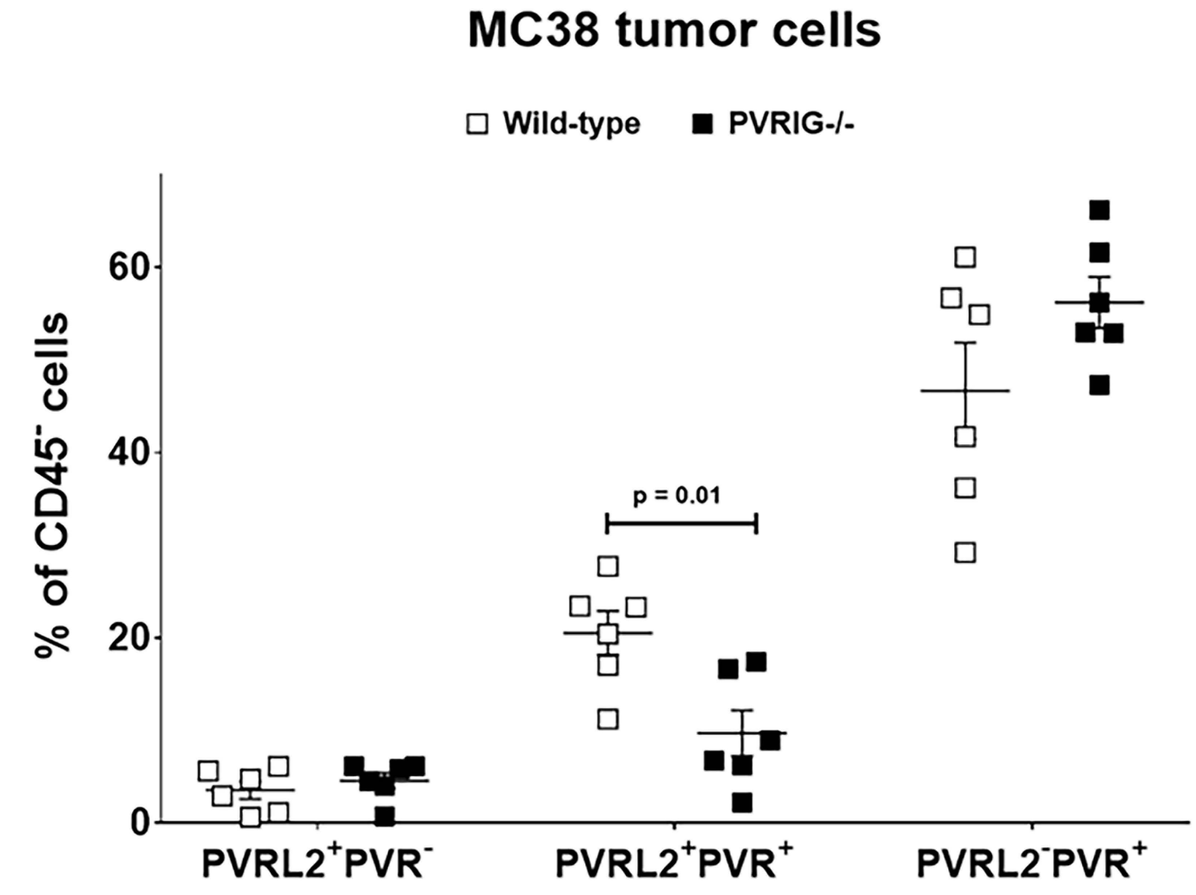

C

PVRIG-/-

Wild-type

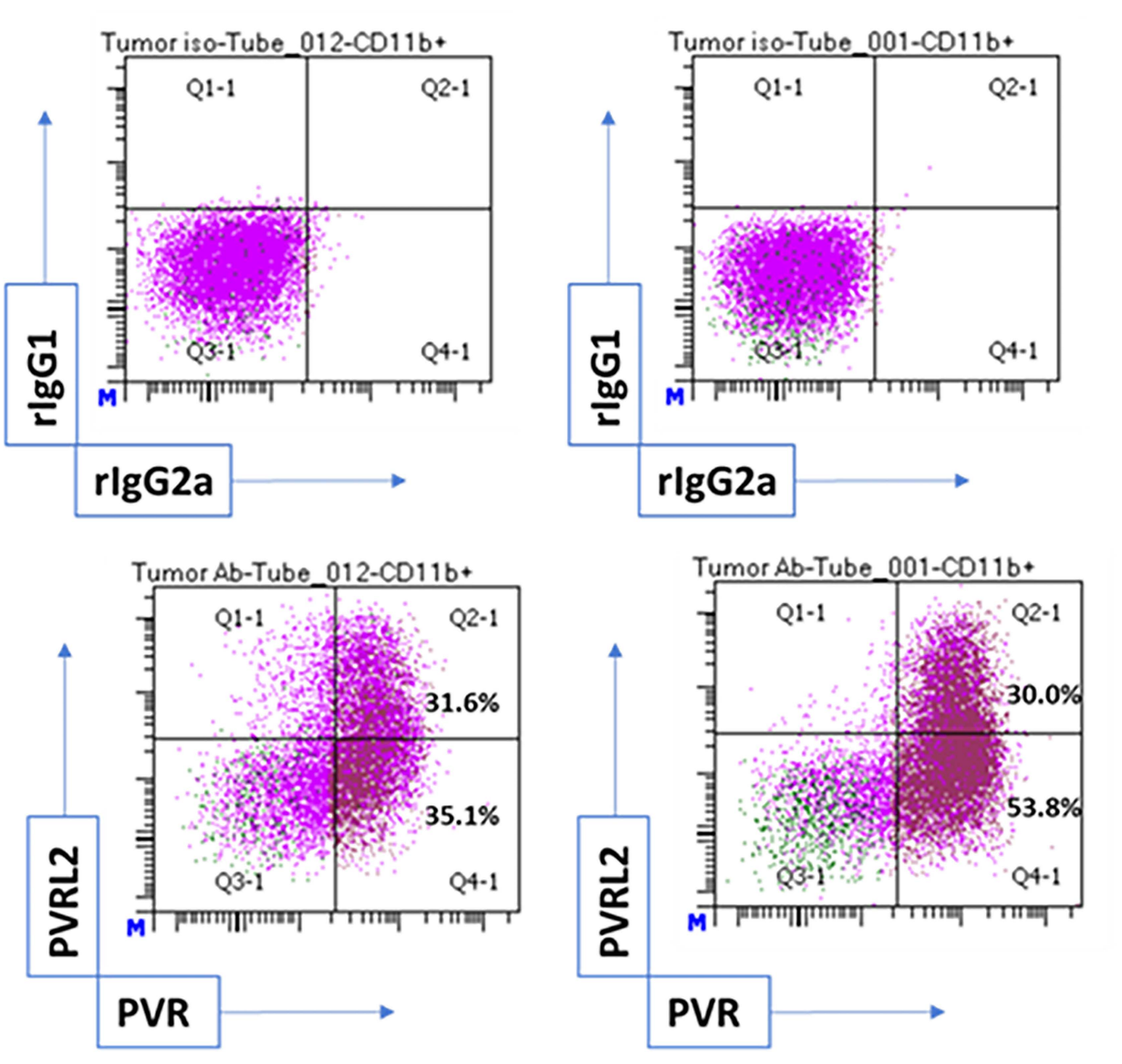

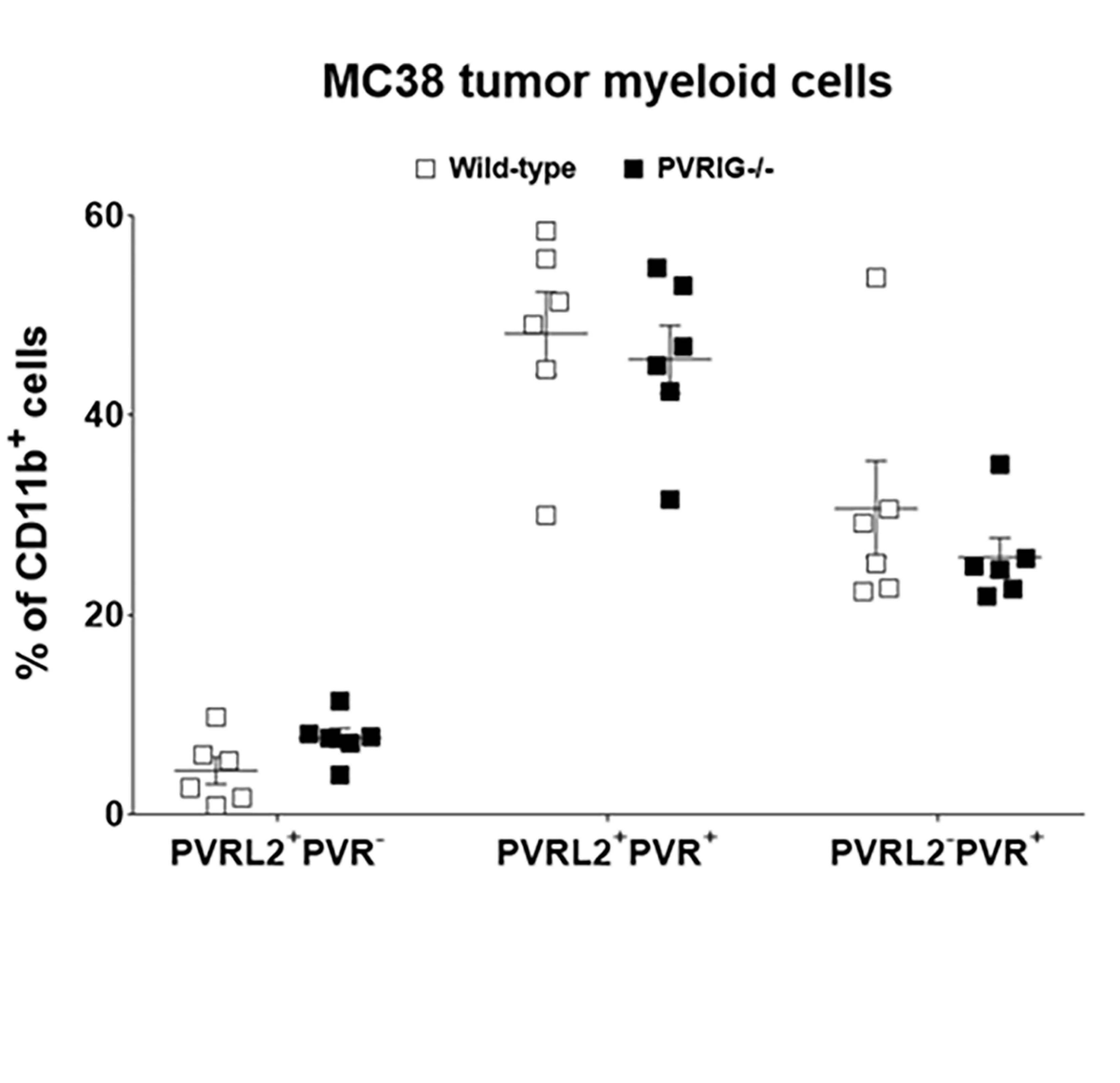

Figure S10

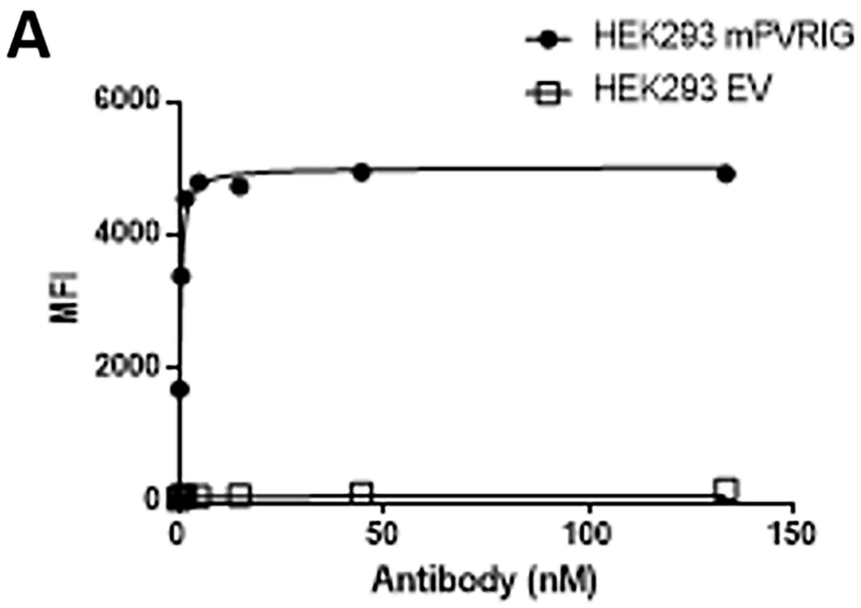
A
HEK293 mPVRIG
HEK293 EV
MFI
6000
4000
2000
0
0
50
100
150
Antibody (nM)

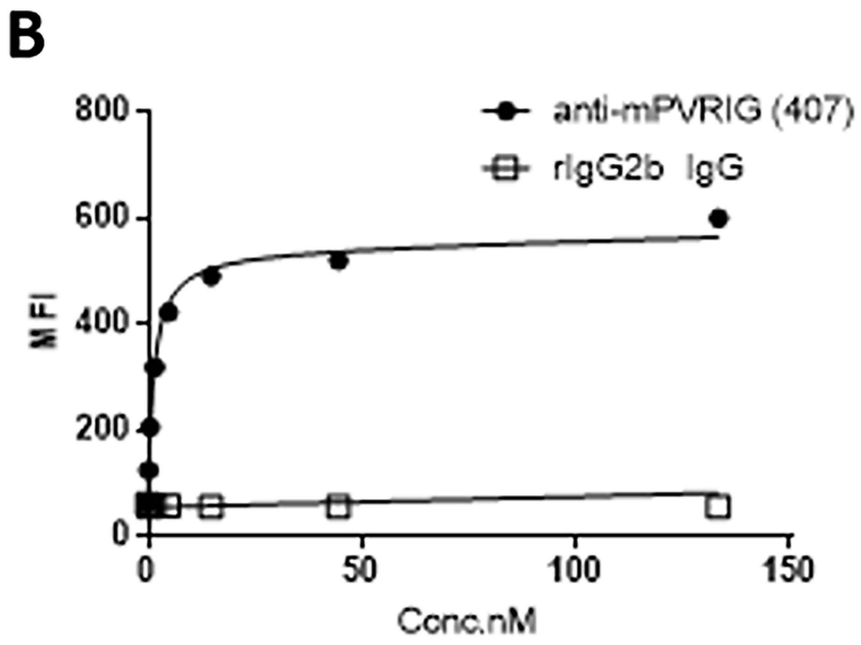
B
anti-mPVRIG (407)
rIgG2b IgG
MFI
800
600
400
200
0
0
50
100
150
Conc.nM

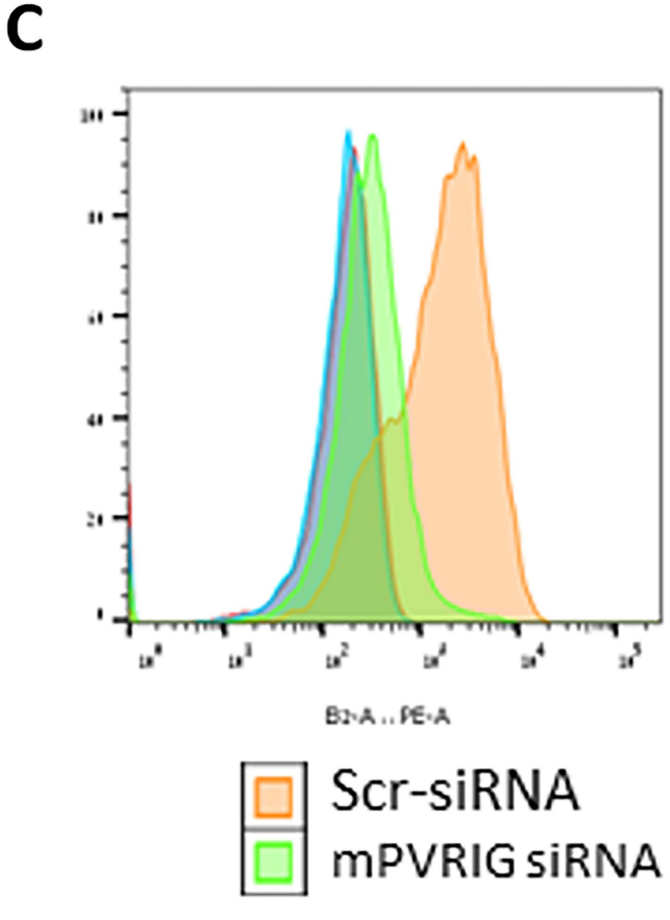
C
Scr-siRNA
mPVRIG siRNA

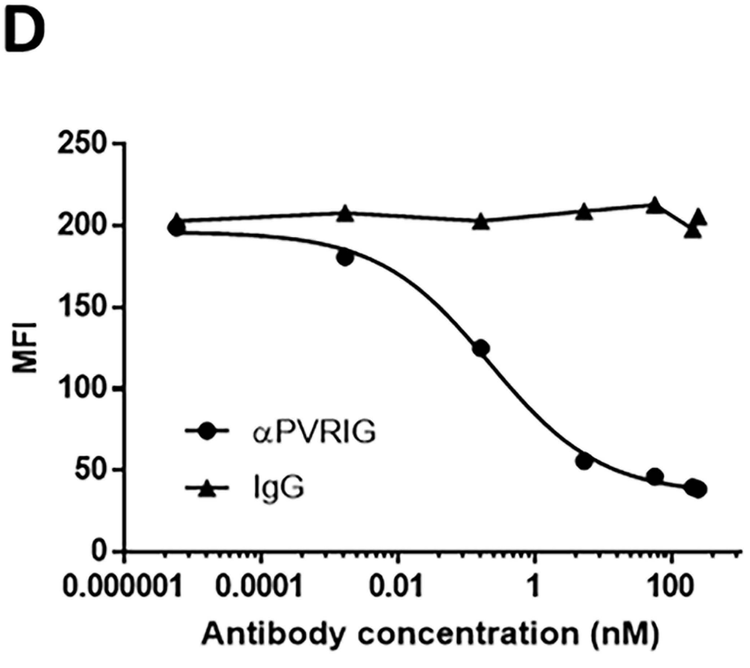
D
MFI
250
200
150
100
50
0
αPVRIG
IgG
0.000001
0.0001
0.01
1
100
Antibody concentration (nM)

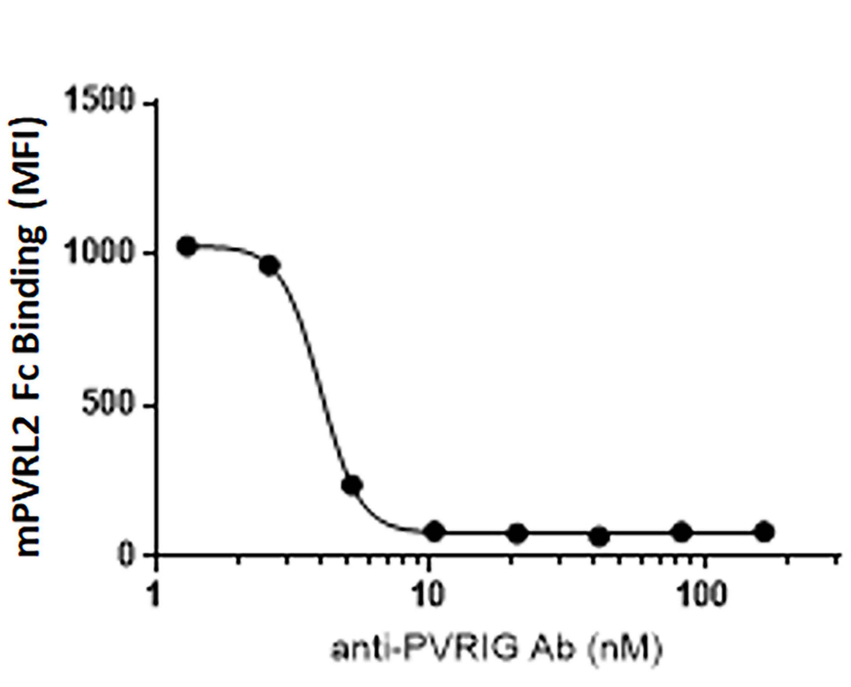
E
mPVRL2 Fc Binding (MFI)
1500
1000
500
0
1
10
100
anti-PVRIG Ab (nM)

Supplementary Figure Legends

Figure S1. Characterization of mPVRIG binding interactions. A-B) Binding of mPVRIG to mPVRL2 was assessed by surface plasmon resonance. C) Soluble receptor (mPVRIG) Fc or control proteins were incubated in a dose response with immobilized mPVRL2 HIS in an ELISA format. Bound receptor Fc is shown. D) Soluble mPVRL2 HIS protein was incubated in a dose response with mPVRIG Fc or mDNAM Fc coated plates. E) Dose titration of recombinant extracellular domains of mouse PVRIG, fused to mouse IgG2a Fc domain, against the mouse PVRL2 extracellular domain or the mouse PVR extracellular domain as recombinant proteins immobilized on EIA plate. F) Binding of mPVRIG Fc or control Fc fusion protein to B16-F10 cell line transfected with mPVRL2 siRNA, mPVR siRNA, or scrambled siRNA transfection is shown. G) Representative overlays illustrate absence of surface PVR (A) and PVRL2 (B) following knockdown with respective siRNAs.

Figure S2. **Generation of PVRIG knockout mice.** The PVRIG conditional knockout mouse line was generated by Ozgene Pty Ltd (Bentley WA, Australia). The targeting construct in which PVRIG exons 1 to 4 were floxed, was electroporated into a C57BL/6 ES cell line, Bruce4. Homologous recombinant ES cell clones were identified by Southern hybridization and injected into goGermline blastocysts. Male chimeric mice were obtained and crossed to C57BL/6J females to establish heterozygous germline offspring on C57BL/6 background. The germline mice were crossed to a ubiquitous FLP C57BL/6 mouse line to remove the FRT flanked selectable marker cassette and generate the conditional allele for PVRIG. Conditional knockout mice were further crossed to a ubiquitous Cre C57BL/6 mouse line to remove the loxP flanked exons and generate the knockout allele.

Figure S3. PVRIG$^{-/-}$ mice are immune-phenotypically similar to wild-type mice. Mice (n= 5 per wild-type and PVRIG knockout cohorts) were euthanized prior to venous blood being collected in anti-coagulant-coated tubes and harvesting of organs. Single cells were recovered from freshly harvested bone marrow, thymus, spleen, cutaneous and mesenteric lymph nodes. Cells were

stained with fluorochrome-conjugated surface marker antibodies and acquired on a BD LSR Fortessa flow cytometer. Panels illustrate comparable frequencies of myeloid cells (A), dendritic cells (B), B cells (C), T cells (D), CD4 T cells (E), CD8 T cells (F), and NK cells (G) across lymphoid tissue types. (H-I) Whole venous blood was run on a Hemavet 950 veterinary hematology system to compare differential counts and frequencies of blood cell subsets from wild-type and PVRIG deficient mice.

Figure S4. PVRIG$^{-/-}$ mice have normal memory CD8^{+} T cell development following immunization with *Listeria monocytogenes*. Wild-type and PVRIG$^{-/-}$ mice were immunized with attenuated Ovalbumin-expressing *Listeria monocytogenes* (LmOVA; 10^6 CFU i.v.). On day 60, mice received a secondary immunization of LmOva (10^7 CFU i.v.). A week later, spleens and hind-limb bone marrow were harvested from the animals and cells were cultured in the absence or presence of Ova 257-264 or Ova 323-339 peptide. Cells were subsequently analyzed for intracellular IFN-γ and TNF-α. Representative dot plots of gated CD8^{+} (top panel) and CD4^{+} (bottom panel) T cells co-producing IFN-γ and TNF-α from spleens (A) and bone marrow (B) of unimmunized / immunized wild-type and PVRIG$^{-/-}$ mice along with graphical summary of cytokine-producing CD8^{+} T cells are shown. Data shown are from two independent experiments. (C) Day 7 SIINFEKL H-2k^{b} tetramer staining of LmOva-immunized and non-immunized wild-type and PVRIG$^{-/-}$ mice. Representative staining dot plots on gated viable CD3^{+}CD4^{-} cells and graphical summary are shown.

Figure S5. B16-F10 tumor growth is inhibited in PVRIG$^{-/-}$ mice. Wild-type and PVRIG$^{-/-}$ mice were implanted with B16-F10 melanoma cells ($2x10^5$ s.c). Tumor volumes were measured bi-weekly beginning on day 11. Average tumor volumes and individual growth curves are presented here.

Figure S6. **CD8 T cell depletion abrogates anti-tumor immunity in PVRIG$^{-/-}$mice.** Wild-type or PVRIG$^{-/-}$ mice were administered 100 μg anti-CD8β (Clone 53-5.8) or rat IgG1 isotype control on the day before as well as on the day of implantation of 5×10^5 MC38 cells and then weekly

thereafter. Tumor volumes were measured twice weekly. n=8/10 mice per group; Ave ± SEM is shown; * p values from a Student's unpaired t-test are shown. Individual tumor growth curves are shown.

Figure S7. Validation of Nanostring gene expression data for select targets by TaqMan qPCR. cDNA was synthesized from RNA extracted from wild-type and PVRIG$^{-/-}$ CD8 TILs and 2 ng of cDNA was used as template in a qPCR reaction with TaqMan gene expression assays for RPL19 (housekeeping gene) and target genes (IFN-γ, Granzyme A, Granzyme B, Perforin, TIGIT, PD-1, CTLA-4, Tim-3 and DNAM-1). ΔCt was calculated for each target relative to RPL19 and the reciprocal (ΔCt^{-1}) values were plotted against the respective Nanostring normalized Log_2 counts.

Figure S8. **TNF-α-producing myeloid cells infiltrate PVRIG-deficient MC38 tumors.** C57BL/6 wild-type or PVRIG$^{-/-}$ mice were subcutaneously implanted with 5×10^5 MC38 cells. At day 18 post-implantation, tumors, spleens, tumor-draining and non-draining lymph nodes were collected from euthanized animals. Dissociated tumors were enriched for CD45$^+$ cells prior to culture for 4 hours with Brefeldin A to trap intracellular cytokines. Representative dot plots show frequencies of TNF-α$^+$ CD11b$^+$ tumor-infiltrating cells from wild-type or PVRIG$^{-/-}$ mice. Accompanying graph shows the percentages of TNF-α$^+$ CD11b$^+$ cells in non-draining lymph nodes, tumor-draining lymph nodes, spleens and tumors from wild-type and PVRIG$^{-/-}$ mice on day 18. Mean ± SEM is shown and p values from a Student's unpaired t-test are shown.

Figure S9. **PVRL2 is induced on tumor-infiltrating myeloid cells.** Day 18 tumors and spleens from wild-type or PVRIG$^{-/-}$ mice were harvested and dissociated cells were analyzed for surface expression of PVRL2 and PVR on CD45$^+$ CD11b$^+$ (myeloid) and CD45$^-$ (tumor) sub-populations. Representative dot plots and graphs show percentages of PVRL2$^+$PVR$^-$, PVRL2$^+$PVR$^+$ and PVRL2$^+$PVR$^-$ subsets within (A) splenic CD11b$^+$ cells, (B) CD45$^-$ tumor cells, and (C) tumoral CD11b$^+$ cells from wild-type and PVRIG$^{-/-}$ mice. Mean ± SEM is shown and p values from a Student's unpaired t-test are shown.

Figure S10. Characterization of a surrogate anti-mPVRIG antibody. A) Affinity characterization of rat anti-mPVRIG mAb was performed by examining the binding of anti-mPVRIG to HEK293 cells overexpressing mPVRIG or control (Empty vector-transfected) HEK293 cells. B) Additional affinity characterization of rat anti-mouse PVRIG mAb was performed by examining binding of anti-mPVRIG to endogenous mPVRIG-expressing D10.G4.1 cell line relative to rat IgG isotype control. C) Binding of anti-mPVRIG to D10.G4.1 cells transfected with mPVRIG-siRNA (green histogram) vs scrambled siRNA (orange histogram). D) Binding of mPVRIG Fc pre-incubated with anti-mPVRIG Ab or rat IgG isotype control to B16-F10 cells, which endogenously express PVRL2. E) Binding of mPVRL2 Fc fusion protein to mPVRIG HEK293 engineered cells that were pre-incubated with serial dilutions of anti-mPVRIG mAb is shown.